Exposure of Epitaxial Graphene on SiC(0001) to Atomic Hydrogen

Nathan P. Guisinger,[1,] Gregory M. Rutter,[2] Jason N. Crain,[1] Phillip. N. First,[2] and Joseph A. Stroscio[1]*

[1,*]Center for Nanoscale Science and Technology, NIST, Gaithersburg, MD 20899

[2]School of Physics, Georgia Institute of Technology, Atlanta, GA 30332

ABSTRACT

Graphene films on SiC exhibit coherent transport properties that suggest the potential for novel carbon-based nanoelectronics applications. Recent studies suggest that the role of the interface between single layer graphene and silicon-terminated SiC can strongly influence the electronic properties of the graphene overlayer. In this study, we have exposed the graphitized SiC to atomic hydrogen in an effort to passivate dangling bonds at the interface, while investigating the results utilizing room temperature scanning tunneling microscopy.

The realization of graphene-based electronics involves numerous challenges that include large-scale device fabrication and the ability to control the electronic properties of the graphene material.[1-10] Since graphene represents a nearly ideal 2D conductor, its electronic properties are very susceptible to the surrounding environment. Variations in the electronic properties are observed depending on whether the graphene exists as a single sheet or as two or more sheets stacked together.[11] In addition, the supporting substrate can affect the graphene.[12,13] It plays a critical role in electrostatic gating and the spatial distribution of charge carriers; essential aspects of electronic devices.[14,15] In this paper, we show the effect of exposing partially-graphitized SiC(0001) to atomic hydrogen in an effort to understand graphene-substrate interactions in this system and potentially to achieve further control of the electronic properties of the graphene overlayer. We study these effects at the atomic-scale using ultra-high vacuum (UHV) scanning tunneling microscopy (STM).

The thermal graphitization of SiC(0001) has so far demonstrated the highest potential for addressing large-scale integration, through epitaxial growth of uniform graphene layers over large areas of the surface.[1,4, 16-18] Transport measurements of epitaxial graphene on SiC(0001) reveal unique properties that are inherent to graphene,[7] although the carrier mobility has yet to match that typically measured for exfoliated graphene or for epitaxial graphene grown on $SiC(000\bar{1})$. Such variations in the measured transport may stem from interactions that occur between the graphene and its supporting substrate. Of particular interest are the interface states that exist on SiC(0001), which may also determine the inherent shift of the Fermi level in epitaxial graphene on SiC(0001), resulting in its n-type doping.[11,12]

The aim of this research is to investigate the character of surface and interface states in the graphene/SiC(0001) system, with a long-term goal of eliminating such states via chemical passivation. We have chosen atomic hydrogen as a probe of the dangling bonds and as a potential passivant. Results from scanning tunneling microscopy and spectroscopy at room temperature demonstrate that silicon dangling bonds in exposed regions of the $6\sqrt{3} \times 6\sqrt{3}R30°$ reconstructed SiC surface are passivated after exposure to atomic hydrogen at an appropriate temperature. The interface reconstruction beneath the first graphene layer is largely unaffected by the same exposure; however

pairwise adsorption of H atoms is observed on the graphene surface, with a subtle long-range effect on the electronic structure.

The graphitization of SiC(0001) involves heating the sample to temperatures in excess of 1200ºC, resulting in the thermal decomposition of the surface.[19] At these temperatures silicon evaporates from the surface, while the remaining carbon atoms undergo diffusion and nucleation to form graphene sheets. As the sample is cooled below the threshold for thermal decomposition, the SiC(0001) surface attempts to minimize its energy by forming a $6\sqrt{3}$ x $6\sqrt{3}R30°$ surface reconstruction,[20] as illustrated in the STM image of Figure 1a. Unsatisfied dangling bonds in this surface reconstruction result in surface states that lie within the bandgap of the SiC(0001),[21] which are apparent given the ability to image the reconstructed surface with tunneling electrons at low energies.

The thermal processing of SiC(0001) allows for a level of control over the amount of graphene that is grown epitaxially on the surface.[8, 20] Figure 1a illustrates a region of $6\sqrt{3}$ x $6\sqrt{3}R30°$ reconstructed SiC(0001) containing no graphene, while Figure 1b shows the transition from a single graphene sheet to a region of SiC(0001)-$6\sqrt{3}$ x $6\sqrt{3}R30°$. Under appropriate tunneling conditions, STM can be used to image the underlying $6\sqrt{3}$ x $6\sqrt{3}R30°$ interface reconstruction below a single graphene sheet.[20, 22] The image of Figure 1b illustrates that the SiC(0001)-$6\sqrt{3}$ x $6\sqrt{3}R30°$ is not limited to graphene-free regions of the surface but also forms uniformly below the graphene (we don't exclude the possibility that the interface reconstruction could differ somewhat from the reconstruction of the graphene-free surface, but we expect that is essentially the same structure).In common practice, hydrogen is used to passivate interface states in traditional silicon-based metal-oxide-semiconductor (MOS) technology.[23, 24] As it is unclear which of the atoms in the SiC(0001)-$6\sqrt{3}$ x $6\sqrt{3}R30°$ surface reconstruction constitute the unsatisfied dangling bonds, it is fortunate that the *in situ* hydrogen passivation of both Si(100)[25] and C(100)[26] is well characterized. For this study, the exposure of graphitized SiC(0001) to atomic hydrogen was performed *in situ* on surfaces that were intentionally prepared with only a fraction of the surface covered by graphene. The samples, 6H-SiC(0001) n-type (ρ = 0.038 Ω-cm^2), were resistively heated to form sub-monolayer graphene. The samples were annealed at various substrate temperatures

and exposed to 0.26 mPa for 600 s (1200 Langmuir) of molecular hydrogen that was cracked on a hot tungsten filament (1400 ºC, approximately 25 cm from the sample), as illustrated in the schematic of Figure 2a . All surfaces were both pre- and post-characterized with STM measurements at room temperature.

Following exposure to hydrogen, the regions of reconstructed SiC(0001)-6√3 x 6√3R30° became difficult to image at sample bias below a magnitude of 2 V and had a disordered appearance suggesting that the dangling bonds were successfully passivated (Figure 2b). However, the underlying 6√3 x 6√3R30° interface appears unchanged over regions of epitaxial graphene (Figure 2b), which suggests that the hydrogen does not reach the SiC interface beneath the graphene layer.

The temperature dependence of the passivation was studied for a range of sample temperatures, while keeping the dose of atomic hydrogen constant. The STM images in Figure 2c show results for four different substrate temperatures. At substrate temperatures below ≈ 400 °C, regions of exposed SiC(0001)-6√3 x 6√3R30° appear to be passivated, while above this temperature they appear unpassivated with the 6√3 x 6√3R30° surface reconstruction clearly visible. For all temperatures studied, the regions containing a graphene overlayer appear unchanged with a well-resolved 6√3 x 6√3R30° interface reconstruction. Apparently, hydrogen diffusion to the interface is impeded at temperatures up to 800 °C. At sample temperatures above ≈ 400 °C the hydrogen is unable to passivate the regions of exposed reconstructed SiC(0001)-6√3 x 6√3R30° due to thermal desorption.

To further verify these interpretations of the topographic data, scanning tunneling spectroscopy (STS) was used to measure the differential conductance over different regions of the surface (Figure 2d). For small tunnel bias, the differential conductance is proportional to the local density of states (LDOS). The differential conductance spectra measured over regions of graphene remained unchanged following exposure to hydrogen and are characteristic of epitaxial graphene, as observed in previous studies.[20, 22] Spectra from the SiC(0001)-6√3 x 6√3R30° shows a narrow bandgap due to the presence of surface states, both prior to passivation and for temperatures exceeding 400 °C. A dramatic difference is observed between spectra acquired over graphene-free regions of unpassivated SiC(0001)-6√3 x

6√3R30° and passivated H:SiC(0001)-6√3 x 6√3R30°. The differential conductance clearly shows a widening of the bandgap to over 1 eV indicating that the hydrogen has in fact passivated the surface states of the SiC(0001)-6√3 x 6√3R30° for temperatures below 400 °C. The loss of these surface states creates an amorphous appearance within the STM images.

Although the passivation of dangling bonds was successful on reconstructed regions of exposed SiC(0001)-6√3 x 6√3R30°, hydrogen did not passivate the interface reconstruction below the first layer of epitaxial graphene. This result is quite surprising considering hydrogen's ability to diffuse through numerous layers and reach the interface of traditional MOS devices. Moreover, because these samples were intentionally prepared with only a fraction of the surface containing epitaxial graphene, one might expect hydrogen to easily diffuse under the graphene layer from its edges. This was not observed. Following passivation, the underlying 6√3 x 6√3R30° interface reconstruction below the graphene is always visible right up to this edge and there is no apparent topographical change at the graphene step edge following passivation. One possible explanation is that the edges of the epitaxial graphene sheets are chemically bound along dangling bonds of the surface reconstruction. This would seal the step edges from hydrogen penetration. This is supported by the STM data, which shows that the edges of the epitaxial graphene form an ordered structure that always terminates along a tetramer row of the underlying surface reconstruction (highlighted by dashed lines in Figure 1b).[20]

Increasing the passivation temperature had little effect on the diffusion of hydrogen below the epitaxial graphene. The temperature-dependent study did show that above 400 °C, hydrogen passivation was very poor on the graphene-free regions of SiC(0001)-6√3 x 6√3R30°, due to thermal desorption. By 800 °C, no passivation was observed. This result is important because it sheds light on the chemical nature of the surface reconstruction. Hydrogen is known to desorb from silicon in the range of 400-500 °C, [25] while desorption from diamond requires temperatures of at least 800 °C. [26] The observed lack of hydrogen on the graphene-free SiC(0001)-6√3 x 6√3R30° substrate at temperatures above 400 °C is consistent with hydrogen adsorption to silicon. Therefore, these results imply that

silicon atoms are responsible for the majority of dangling bonds within the surface reconstruction, even though the reconstruction itself is thought to be carbon-rich.

Although we find no passivation of interface states below the graphene monolayer, hydrogen does adsorb to the surface of graphene, as shown in Figure 3. The observed hydrogen coverage on regions of graphene is very low, considering that the same dose completely passivates the non-graphitized regions. Upon closer inspection (Figure 3b), the individual adsorption sites of atomic hydrogen are topographically consistent with recent studies of the adsorption of hydrogen and deuterium on graphite,[27-29] and with theoretical studies of hydrogen on graphene.[30] These studies of carbon-based materials for hydrogen storage have shown that the initial adsorption of atomic hydrogen/deuterium to graphite occurs as H-atom pairs. Electronically, hydrogen-atom adsorption introduces some sp^3-character into the local sp^2-bonds; a configuration that may be stabilized by an adjacent H-graphene complex.[27-30] In this study, hydrogen adsorption to graphene was investigated at passivation temperatures of 377 °C or below.

The two most energetically favorable binding sites for hydrogen pair formation on graphite are on opposite sides of the hexagonal ring [Figure 4a(i)] and as two nearest neighbors [Figure 4a(ii)].[27, 28] These sites are also the most energetically favorable on graphene, as confirmed with our STM measurements. Figure 4b shows a representative high resolution image acquired over a hydrogen pair. The pairs exhibit a strong bias dependence in topographic images, and at certain sample biases the individual hydrogen atoms within a pair can be resolved (Figure 4c). Consequently, we can distinguish pairs formed on nearest-neighbor carbon atoms (top left of Figure 4c) and those formed on opposite sides of the hexagon (bottom right of Figure 4c).

It may not be surprising that the hydrogen adsorption pathway on graphene would be similar to that of graphite, but this result does indicate that the first layer of graphene grown epitaxially on SiC(0001)-6√3 x 6√3R30° has sp^2-bonding, as the hydrogen would otherwise not adsorb to it. Further measurements show that hydrogen adsorption alters the local electronic properties of epitaxial graphene on SiC(0001)-6√3 x 6√3R30°, which is quite unexpected and different from adsorption on graphite.[27-29]

Figure 4d shows seven different hydrogen pairs highlighted by blue and white circles (corresponding to bright and dim H-induced topographic features). As previously mentioned, there is a strong bias dependence in the topographic images of hydrogen adsorbed to epitaxial graphene. The bias dependent variations in these images are not localized to the hydrogen but extend over a large area surrounding the pairs, as illustrated in the filled-states image of Figure 4e. It appears that hydrogen adsorption reduces the local density of states (darker regions). Thus hydrogen adsorption may be used to locally change the carrier concentration in graphene.

In summary, single graphene sheets were grown epitaxially on SiC(0001)-$6\sqrt{3}$ x $6\sqrt{3}R30°$ and exposed to atomic hydrogen in an effort to passivate surface and interface states, and alter the electronic properties of epitaxial graphene in a controlled way. Passivation of the graphene-free regions of SiC(0001)-$6\sqrt{3}$ x $6\sqrt{3}R30°$ was successful, but hydrogen did not diffuse through the graphene monolayer, suggesting that the edge of the graphene is chemically bound to the reconstructed SiC(0001)-$6\sqrt{3}$ x $6\sqrt{3}R30°$ surface. In addition, hydrogen adsorption to epitaxial graphene was investigated experimentally for the first time, and the atomic-scale imaging of individual hydrogen atoms confirmed the formation of H-atom pairs, as observed previously for deuterium on graphite. Unlike graphite, hydrogen adsorption results in a dramatic change in the local density of states over a spatial region much larger than the atomic adsorption sites.

FIGURE CAPTIONS

Figure 1. (a) Topographic image of the $6\sqrt{3}$ x $6\sqrt{3}R30°$ surface reconstruction of 6H-SiC(0001) (imaging conditions: sample bias +2 V, tunneling current 0.1 nA). (b) Atomic-resolution image showing the registration of a graphene edge (orange) with the SiC(0001)-$6\sqrt{3}$ x $6\sqrt{3}R30°$ surface and interface reconstructions (imaging conditions: sample bias +1 V, tunneling current 0.1 nA). Dashed white lines highlight the positions of adjacent tetramer rows of the reconstructions. The edge of the graphene appears to be perfectly aligned with the tetramer row and has an ordered appearance along its edge. From images of the graphene lattice, the graphene step edge has armchair alignment.

Figure 2. (a) Schematic representation of molecular hydrogen being cracked on hot tungsten filament that is in line of sight with the sample. (b) STM image of the surface following exposure to hydrogen at a sample passivation temperature of 377 °C. The region of monolayer graphene (lower right) appears unchanged by H-exposure, and the underlying $6\sqrt{3}$ x $6\sqrt{3}R30°$ interface reconstruction remains. No regions of graphene-free $6\sqrt{3}$ x $6\sqrt{3}R30°$ surface reconstruction remain on the sample, but disordered regions (left and top of image) abut the graphene terraces, indicating substantial reaction of hydrogen with the graphene-free regions, but no reaction in graphitized regions (imaging conditions: sample bias +2 V, tunneling current 0.1 nA). (c) Temperature dependence of hydrogen passivation. For temperatures below 400 °C the regions of exposed SiC(0001) are passivated, but above 600 °C the SiC(0001) appears relatively unreactive. (d) Differential conductance measured over the regions of interest. The 1.5 eV bandgap in the spectrum (blue) verifies that surface states of the exposed SiC(0001) are passivated.

Figure 3. (a) STM image showing several hydrogen adsorption sites on monolayer graphene that appear as dark spots distributed randomly over the graphene surface (imaging conditions: sample bias +2 V, tunneling current 0.1 nA). (b) Higher resolution topograph (area outlined by black box in (a)) of over individual adsorption sites (imaging conditions: sample bias +1 V, tunneling current 0.1nA).

Figure 4. (a) The two most energetically favorable configurations for hydrogen pair formation are when the atoms are on opposite sides of the hexagonal ring (a(i)) or when they are adjacent (a(ii)). (b) For some tunneling biases the individual hydrogen atoms within the pair can be resolved, as highlighted by the white arrows (sample bias +0.8 V). (c) The hydrogen pair adsorption sites are distinguished in this STM image. The top-left pair appears to be hydrogen atoms on adjacent carbon sites, (a(i)), and the bottom-right pair of H atoms are found on opposite sides of a graphene hexagon, (a(ii)). Black hexagons have been overlaid for clarity. (d) STM image of seven different hydrogen pairs highlighted with blue and white circles (imaging conditions: sample bias + 2V, tunneling current 0.1 nA). Hydrogen pairs within the blue circles are uniformly brighter than those in the white circles. The difference is as yet unexplained (we note that the features occur at similar positions on the graphene relative to the underlying SiC reconstruction). (e) The same area imaged at a sample bias of -1.0 V reveals a dramatic change in the LDOS that is delocalized over an extended area in the vicinity of the hydrogen pairs (highlighted with black outline).

REFERENCES

1. Geim, A. K.; Novoselov, K. S. *Nature Mat.* **2007**, 6, 183.

2. Novoselov, K. S.; Geim, A. K.; Morozov, S. V.; Jiang, D.; Zhang, Y.; Dubonos, S. V.; Grigorieva, I. V.; Firsov, A. A. *Science* **2004,** 306, 666.

3. Novoselov, K. S.; Jiang, D.; Schedin, F.; Booth, T. J.; Khotkevich, V. V.; Morozov, S. V.; Geim, A. K. *Proc. Natl. Acad. Sci. USA* **2005,** 102, 10451.

4. Berger, C.; Song, Z. M.; Li, T. B.; Li, X. B.; Ogbazghi, A. Y.; Feng, R.; Dai, Z. T.; Marchenkov, A. N.; Conrad, E. H.; First, P. N.; de Heer, W. A. J. *Phys. Chem. B* **2004**, 108, 19912.

5. Novoselov, K. S.; Geim, A. K.; Morozov, S. V.; Jiang, D.; Katsnelson, M. I.; Grigorieva, I. V. ; Dubonos, S. V. ; Firsov, A. A. *Nature* **2005**, 438, 197.

6. Zhang, Y. B.; Tan, Y. W.; Stormer, H. L.; Kim, P. *Nature* **2005**, 438, 201.

7. de Heer, W. A.; Berger, C.; Wu, X. S.; First, P. N.; Conrad, E. H.; Li, X. B.; Li, T. B.; Sprinkle, M.; Hass, J.; Sadowski, M. L.; Potemski, M.; Martinez, G. *Solid State Communications* **2007**, 143, 92.

8. Berger, C.; Song, Z. M.; Li, X. B.; Wu, X. S.; Brown, N.; Naud, C.; Mayou, D.; Li, T. B.; Hass, J.; Marchenkov, A. N.; Conrad, E. H.; First, P. N.; de Heer, W. A. *Science* **2006**, 312, 1191.

9. Novoselov, K. S. ; Jiang, Z.; Zhang, Y.; Morozov, S. V.; Stormer, H. L.; Zeitler, U.; Maan, J. C.; Boebinger, G. S.; Kim, P.; Geim, A. K. *Science* **2007**, 315, 1379.

10. Zhang, Y.; Jiang, Z.; Small, J. P.; Purewal, M. S.; Tan, Y. W.; Fazlollahi, M.; Chudow, J. D.; Jaszczak, J. A.; Stormer, H. L.; Kim, P. *Phys. Rev. Lett.* **2006**, 96, 136806.

11. Ohta, T.; Bostwick, A.; Seyller, T.; Horn, K.; Rotenberg, E. *Science* **2006**, 313, 951.

12. Zhou, S. Y.; Gweon,G. H.; Fedorov, A. V.; First, P. N.; De Heer, W. A.; Lee, D. H.; Guinea, F.; Neto, A. H. C.; Lanzara, A. *Nature Mat.* **2007**, 6, 770.

13. Chen, J. H.; Jang, C.; Xiao, S. D.; Ishigami, M.; Fuhrer, M. S. *Nature Nano.* **2008**, 3, 206.

14. Oostinga, J. B.; Heersche, H. B.; Liu, X. L.; Morpurgo, A. F.; Vandersypen, L. M. K. *Nature Mat.* **2008**, 7, 151.

15. Chen, J. H. ; Jang, C.; Adam, S.; Fuhrer, M. S.; Williams, E. D.; Ishigami, M. *Nature Physics* **2008**, 4, 377.

16. Owman, F.; Martensson, P. *Surf. Sci.* **1995**, 330, L639.

17. Owman, F.; Martensson, P. *J. Vac. Sci. & Tech. B* **1996**, 14, 933.

18. Martensson, P.; Owman, F.; Johansson, L. I. *Phys. Stat. Sol. B* **1997**, 202, 501.

19. van Bommel, A. J.; Crombeen, J. E.; van Tooren, A. *Surf. Sci.* **1975**, 48, 463.

20. Rutter, G. M.; Guisinger, N. P.; Crain, J. N.; Jarvis, E. A. A.; Stiles, M. D.; Li, T.; First, P. N.; Stroscio, J. A. *Phys. Rev. B* **2007,** 76, 235416.

21. Emtsv, K. V.; Speck, F.; Seyller, Th.; Ley, L.; Riley, J. D. *Phys. Rev. B* **2008**, 77, 155303.

22. Rutter, G. M.; Crain, J. N. Guisinger, N. P.; Li, T.; First, P. N.; Stroscio, J. A. *Science* **2007**, 317, 219.

23. Cartier, E.; Stathis, J. H.; Buchanan, D. A. *Appl. Phys. Lett.* **1994**, 63, 1510.

24. Fowler, A. B. U.S. Patent 3 849 204, **1974**.

25. Hersam, M. C.; Guisinger, N. P.; Lee, J.; Cheng, K. G.; Lyding, J. W. *Appl. Phys. Lett.* **2002**, 80, 201.

26. Bobrov, K.; Mayne A.; Comtet, G.; Dujardin, G.; Hellner, L.; Hoffman A. *Phys. Rev. B* **2003**, 68, 195416.

27. Hornekaer, L.; Sljivancanin, Z.; Xu, W.; Otero, R.; Rauls, E.; Stensgaard, I.; Laegsgaard, E.; Hammer, B.; Besenbacher, F. *Phys. Rev. Lett.* **2006**, 96, 156104.

28. Hornekaer, L.; Rauls, E.; Xu, W.; Sljivancanin, Z.; Otero, R.; Stensgaard, I.; Laegsgaard, E.; Hammer, B.; Besenbacher, F. *Phys. Rev. Lett.* **2006**, 97, 186102.

29. Andree, A.; Le Lay, M.; Zecho, T.; Kupper, J. *Chem. Phys. Lett.* **425**, 99-104 (2006).

30. Boukhvalov, D. W.; Katsnelson, M. I.; Lichtenstein, A. I. *Phys. Rev. B* **2008**, 77, 035427.
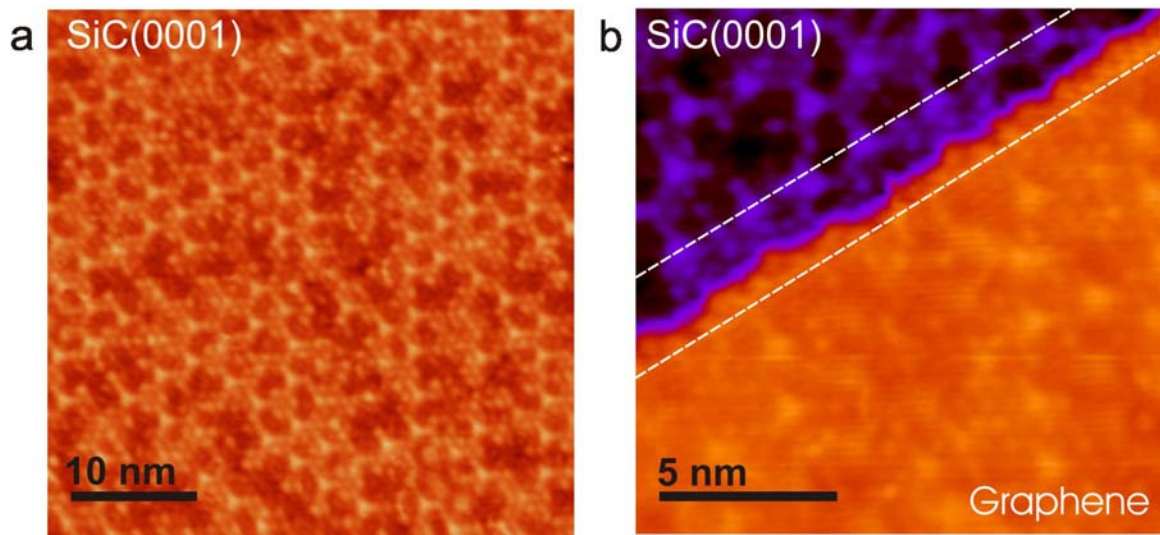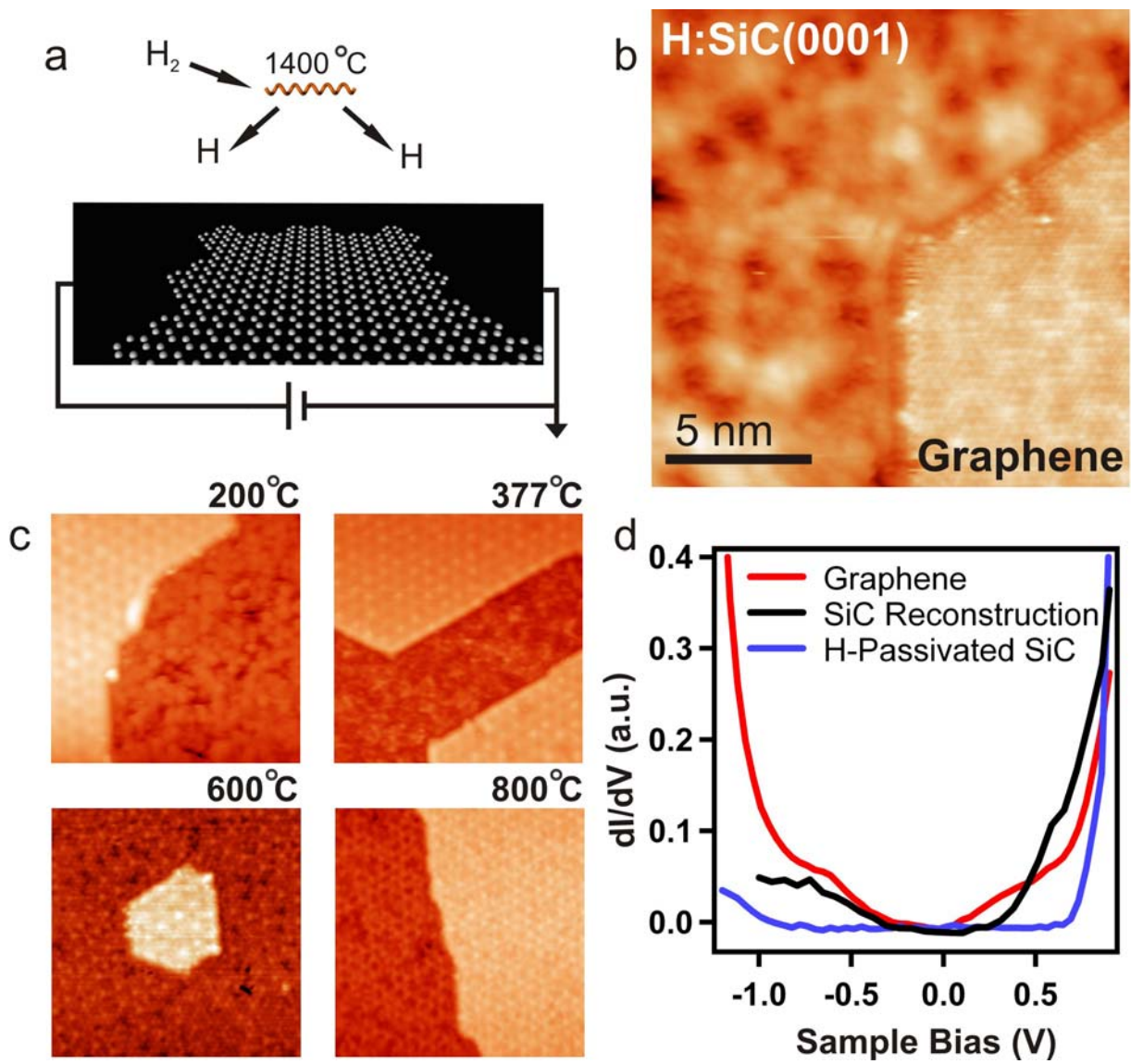
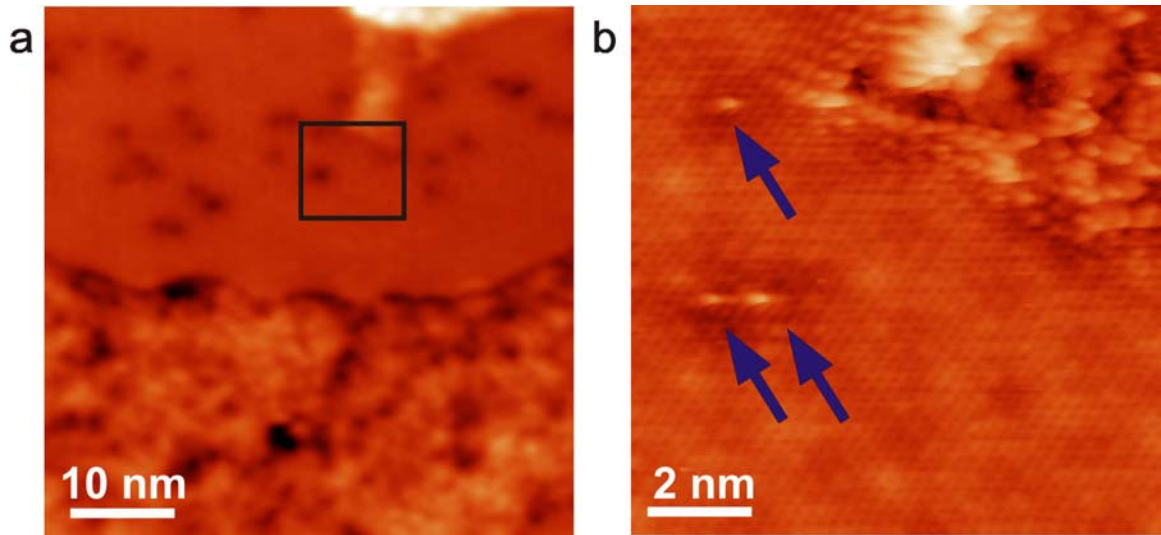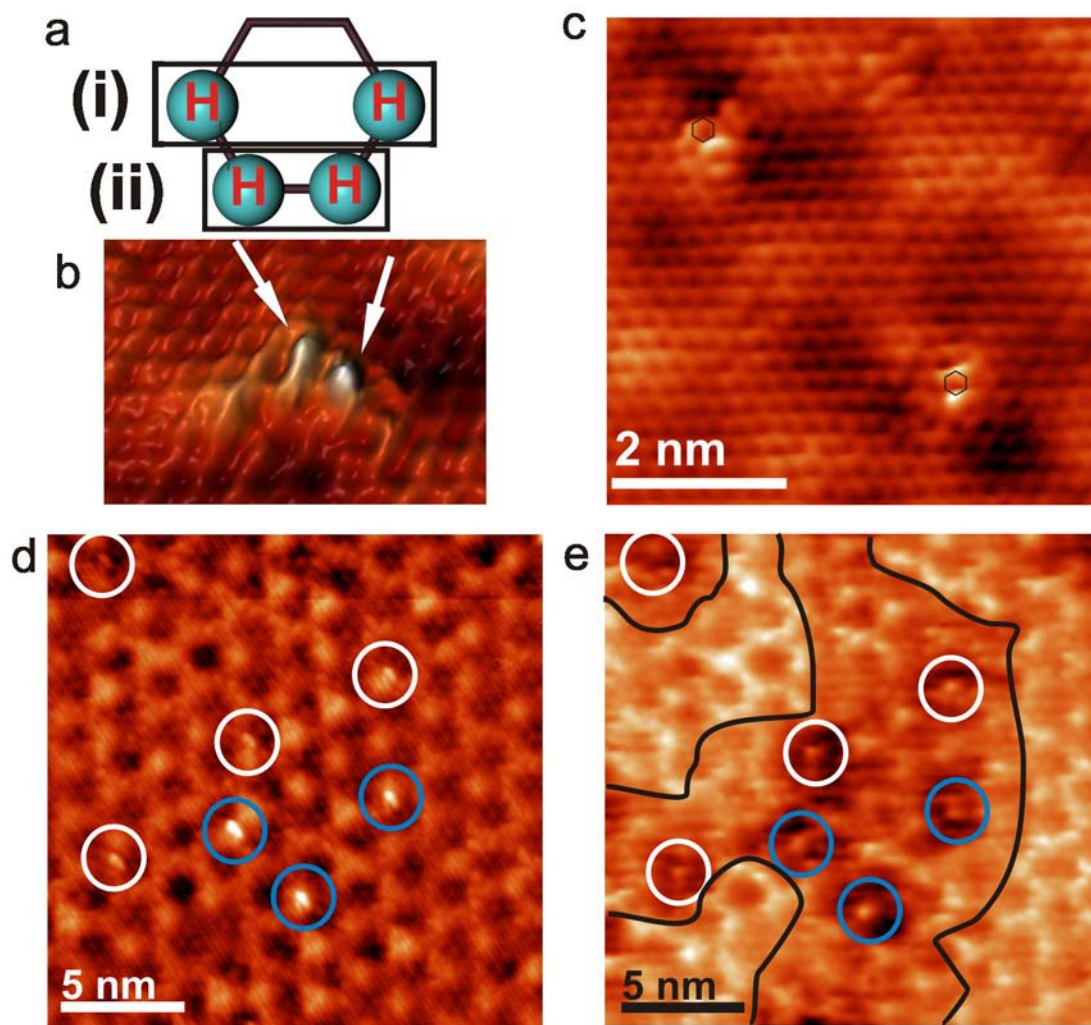Figure 1, N. P. Guisinger *et al.*

Figure 2, N. P. Guisinger *et al.*

Figure 3, N. P. Guisinger *et al.*

Figure 4, N. P. Guisinger *et al.*